17th IEEE International Conference on Advanced Thermal Processing of Semiconductors-RTP 2009

22nm Node n+ SiC Stressor Using Deep PAI+C_7H_7+P_4 With Laser Annealing

John Borland[1], Masayasu Tanjyo[2], Nariaki Hamamoto[2], Tsutomu Nagayama[2], Shankar Muthukrishnan[3], Jeremy Zelenko[3], Iad Mirshad[4], Walt Johnson[4], Temel Buyuklimanli[5], Hiroshi Itokawa[6], Ichiro Mizushima[6] and Kyoichi Suguro[6]

1) J.O.B. Technologies, Aiea, HI
2) Nissin Ion Equipment, Kyoto, Japan
3) Applied Materials, Sunnyvale, CA
4) KLA-Tencor, San Jose, CA
5) EAG, Sunnyvale, CA
6) Toshiba Corporation, Yokohama, Japan

e-mail: JohnOBorland@aol.com

***Abstract*-We investigated n+SiCP stressors formation by C & P implantation with various amorphization techniques and using high temperature laser annealing SPE technique. Both monomer C and molecular C (C_7H_7) with P_4 implant doping was compared as well as with pre-amorphizing implants (PAI) using Ge, Xe or Sb to enhance the Csub level through SPE amorphous layer regrowth. A P dopant activation level of 4E20/cm^3 and a Csub level of 1.52% for Sb-PAI+C_7+P_4 was realized with s strain layer depth of 50nm using a 1325^{o}C peak laser anneal temperature.**

INTORDUCTION

Global Foundries recently announced on July 24, 2009 that they will implement eSiC stressor for nMOS at 22nm node [1]. Using in-situ P doped selective SiC epi this technique is reported to be expensive due to very low growth rate of <2wph and process integration challenges to avoid RTA and implantation induced Csub degradation [2,3]. An alternative is to use C-implantation into an amorphous layer followed by SPE regrowth technique to achieve >1% Csub as reported by Liu et al. from IBM [4]. Since that report others have reported on using both monomer C and molecular C (C_7 or C_{14}) [5-8]. One of the advantages of using C_7 is it is self-amorphizing thereby avoiding the need for a separate Ge-PAI implant step which creates EOR (end-of-range) defects and Ge incorporation into the silicon lattice (larger atom than Si) leading to compressive strain that would compensate the C tensile strain. The periodic table is shown in Fig.1. Another problem is the n+ doping process competes for the same substitutional lattice sites as C but P is preferred over As or Sb having the smallest atom size and neutral strain in Si. Therefore in this paper we will report on our study to examine all these effects by comparing monomer C to C_7 for self-amorphization effects as well as using an additional Ge, Xe or Sb PAI step to control deeper amorphization. The Xe and Sb amorphous dose (5E13/cm^2) is 10x lower than Ge amorphous dose (5E14/cm^2) and Xe being inert will not compete for substitutional lattice site.

EXPERIMENTATION

P-type 300mm wafers were used in this study and all the implants were done at Nissin using the Claris molecular dopant implanter. P_4 was used for the n+ phosphorus doping at 12keV and 5E14/cm^2 dose for a P equivalent of 3keV and 2E15/cm^2 dose. Half the wafers received C doping by monomer C implantation at 3keV/6E14/cm^2 dose and 10keV/3.7E15/cm^2 dose and the remaining wafers were C doped using C_7H_7 implantation at 22.8keV/8.6E13/cm^2 dose and 75.8keV/5.3E14/cm^2 dose. Ge is a row 4 element shown in the periodic table in Fig.1 so the PAI implant condition selected was 40keV/5E14/cm^2 dose to achieve a 60nm deep amorphous layer. For comparison both Sb and Xe (row 5 elements) PAI conditions were 60keV/5E13/cm^2 dose resulting in a 50nm deep amorphous layer as shown in the X-TEM image of Fig.2 and the amorphous depth versus implant energy chart in Fig.3. Fig.4 shows the various implant conditions used in this study. All the wafers were sub-melt laser annealed at Applied Materials using the DSA laser system without capping layer at 4 different peak temperatures as shown in Fig.5 (1175^{o}C, 1225^{o}C, 1275^{o}C and 1325^{o}C).

Fig.1: Periodic table of elements showing C, Ge, Sb and Xe.

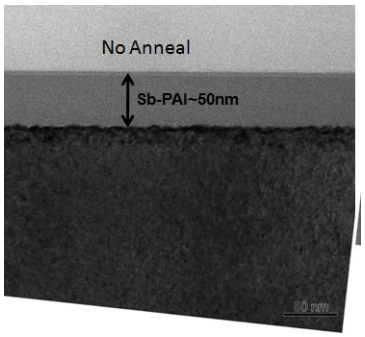

Fig.2: X-TEM of Sb-PAI no anneal region showing 50nm deep amorphous layer for 60keV/5E13/cm^2 implant.

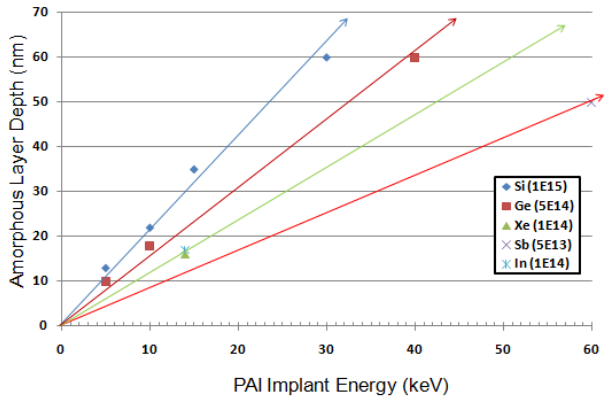

Fig.3: Amorphous depth versus PAI implant energy, species and dose.

Slot No.	Cond. No.	PAI Ion	PAI Energy (keV)	PAI Dose (/cm2)	C Ion	C Energy (keV)	C Dose (/cm2)	P Ion	P Energy (keV)	P Dose (/cm2)	Tilt (deg)	Twist (deg)	Anneal (°C)
1	a	-	-	-	C	3/10	6E14+3.7E15	P4	12	5.00E+14	0	0	
													1225
													1275
													1325
2	b	-	-	-	C7	22.8/75.8	8.6E13+5.3E14	P4	12	5.00E+14	0	0	1175
													1225
													1275
													1325
4	d	Ge	40	5.00E+14	C	3/10	6E14+3.7E15	P4	12	5.00E+14	0	0	1175
													1225
													1275
													1325
5	e	Xe	60	5.00E+13	C	3/10	6E14+3.7E15	P4	12	5.00E+14	0	0	1175
													1225
													1275
													1325
6	f	Sb	60	5.00E+13	C	3/10	6E14+3.7E15	P4	12	5.00E+14	0	0	1175
													1225
													1275
													1325
8	h	Ge	40	5.00E+14	C7	22.8/75.8	8.6E13+5.3E14	P4	12	5.00E+14	0	0	1175
													1225
													1275
													1325
9	i	Xe	60	5.00E+13	C7	22.8/75.8	8.6E13+5.3E14	P4	12	5.00E+14	0	0	1175
													1225
													1275
													1325
10	j	Sb	60	5.00E+13	C7	22.8/75.8	8.6E13+5.3E14	P4	12	5.00E+14	0	0	1175
													1225
													1275
													1325

Fig.4: Experimental matrix conditions for implants.

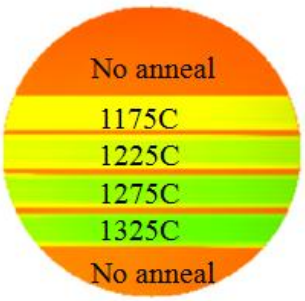

Fig.5: TW full wafer image showing the 4 different laser annealing temperature regions and no anneal regions.

RESULTS

PCOR-SIMS depth profiles were conducted at EAG in New Jersey. The as-implanted profiles from the no annealed regions are shown in Fig.6, note the as implanted P junction depth (Xj) varies between 19.2-19.7nm showing no evidence of P channeling while after the 1325°C laser anneal Xj was ~20.5-22.3nm as shown in Fig.7. The deep tail in the C depth profile for the monomer C without PAI due to C channeling reaches 1E19/cm^3 level at 129nm depth. C_7 without PAI also shows channeling but about 20nm less with a 1E19/cm^3 C level at 110nm depth. With Ge, Xe or Sb PAI both monomer C and C_7 show no channeling and a 1E19/cm^3 C level is achieved at a depth of 81nm. From a process integration point of view the C depth profile will be limited based on the gate stack height because the deep C profile tail must not extend or penetrate through the gate electrode into the gate dielectric material and channel below as reported by Nishikawa et al. [9]. Shallower C profiles with precise amorphous depth to control the Csub strain layer thickness is critical.

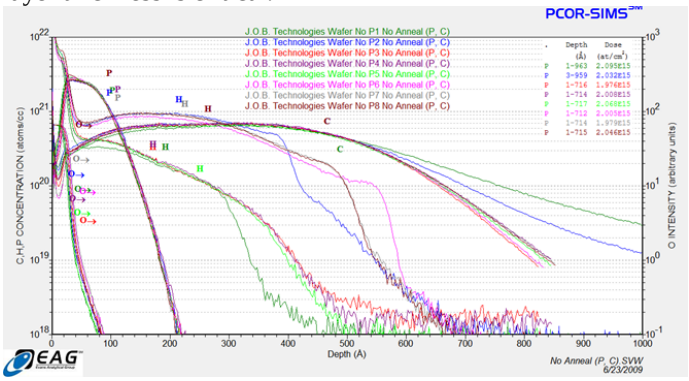

Fig.6: P & C PCOR-SIMS depth profiles in the no anneal region.

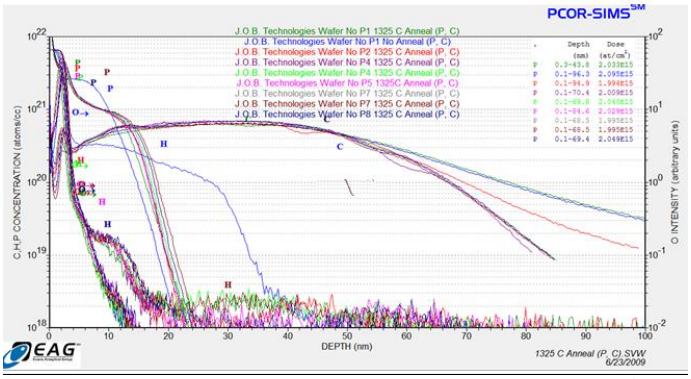

Fig.7: P & C PCOR-SIMS depth profiles in the 1325°C anneal region.

Sheet resistance (Rs) results are shown in Fig.8. Note that for the C+P_4 case, Rs was not dependent on peak laser annealing temperature, all the other cases showed a strong dependence of Rs with laser peak annealing temperature up to 1275°C. This might be related to C substitutional level (Csub) since the C+P_4 had the lowest Csub level as will be discussed later in Fig.16. To achieve low Rs the laser peak temperature needs to be >1275°C. Fig. 9 shows the Rs versus Xj chart for this work showing a P dopant activation solid solubility (Pss) level of >4E20/cm^3.

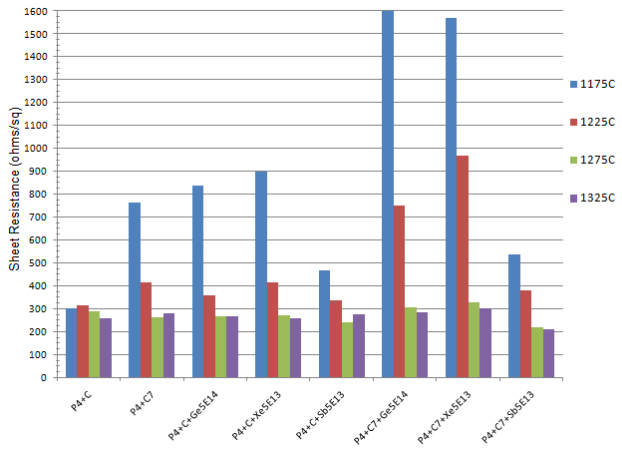

Fig.8: Sheet resistance (Rs) results.

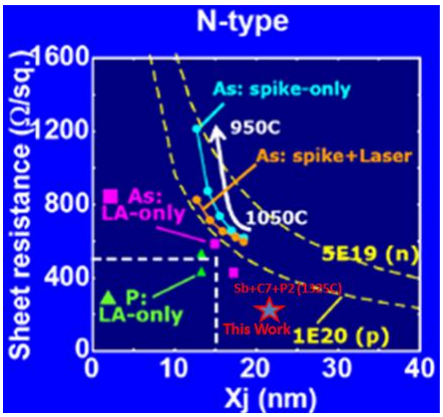

Fig.9: Rs versus Xj chart showing Pss~4E20/cm^3.

Thermal-wave (TW) analysis was used to detect residual implant damage after the various anneals and implant conditions as shown in Fig. 10. C_7 shows less residual implant damage after anneal (TW=4350) compared to monomer C (TW=5500) especially for the higher anneal temperatures. Xe-PAI also had the highest TW value after anneal (TW=5750) followed by Sb-PAI (TW=4150) and then Ge-PAI (TW=3750).

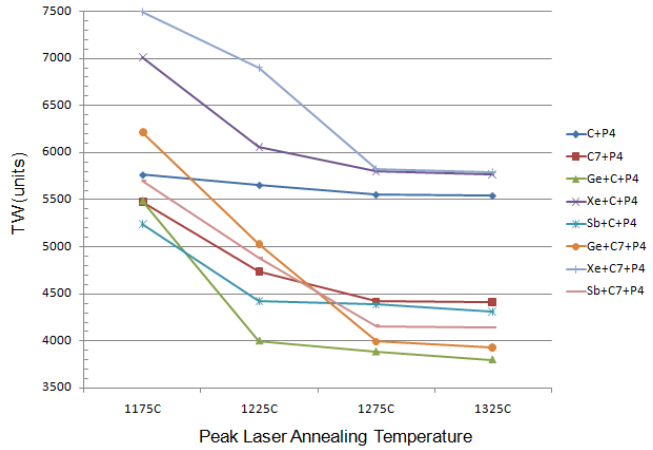

Fig.10: TW results to detect the level of residual implant damage after the various anneals.

The X-TEM results are shown in Fig.11 a-e. These are all after the 1325°C peak temperature laser anneal. The end-of-range (EOR) damage can clearly be detected beyond the original amorphous layer interface. For C+P_4 the EOR damage is ~40nm deep, for C_7+P_4 EOR damage is ~50nm deep, for Ge-PAI+C+P_4 EOR damage is ~65nm deep, for Xe-PAI+C_7+P_4 EOR damage is ~65nm deep and for Sb-PAI+C_7+P_4 EOR damage is ~60nm deep. Also note the evidence of surface stacking faults in the top 10nm of the surface because a 1keV C implant was missing from this study resulting in the surface drop of C profile in the PCOR-SIMS shown in Figs. 6 & 7. The laser anneal SPE regrowth rate increases as the C profile drops off near the surface and this has been reported to give rise to near surface defects and stacking faults as we also observed in this study [6].

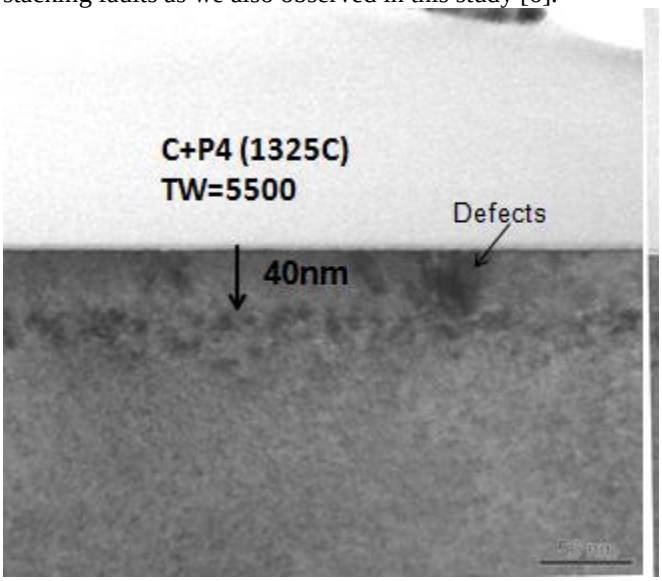

Fig.11a: C+P_4 1325°C anneal.

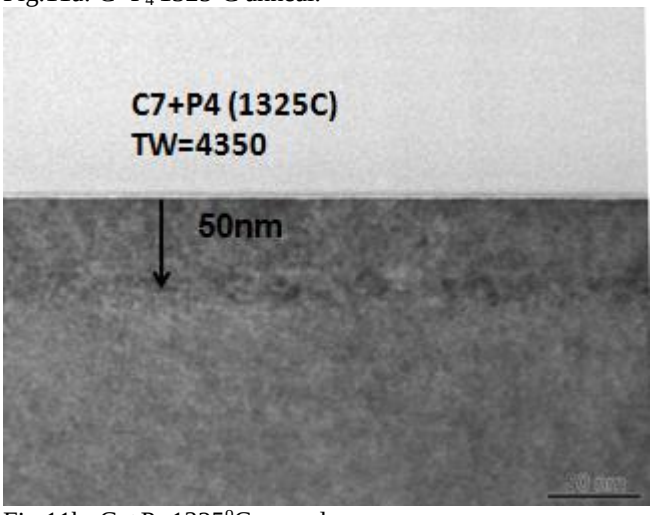

Fig.11b: C_7+P_4 1325°C anneal.

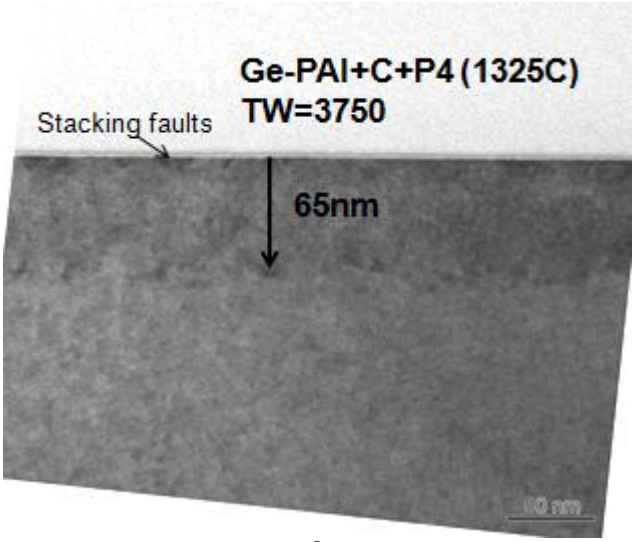

Fig.11c: Ge-PAI+C+P_4 1325°C anneal.

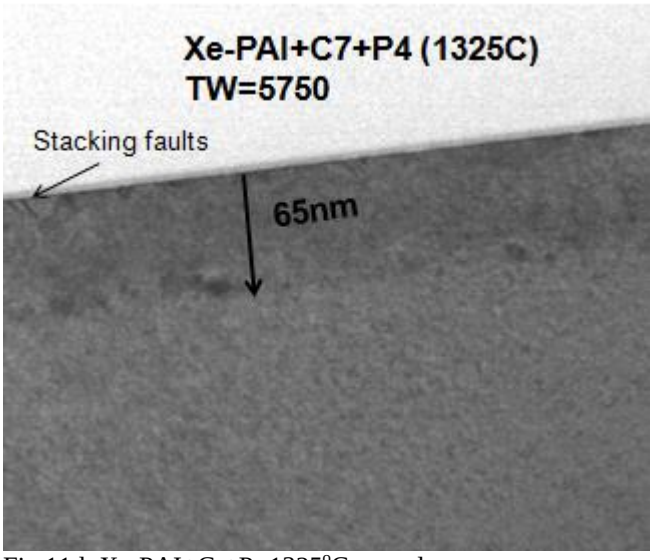

Fig.11d: Xe-PAI+C_7+P_4 1325°C anneal.

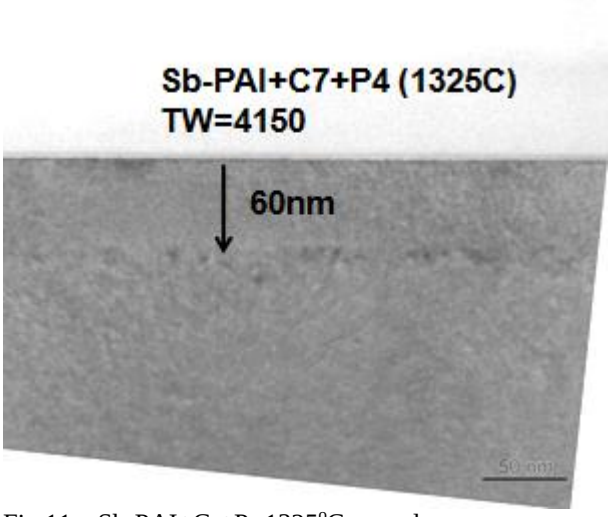

Fig.11e: Sb-PAI+C_7+P_4 1325°C anneal.

XRD rocking curve analysis was conducted for each different laser peak temperature annealing split condition by Toshiba and the results are shown in Figs. 12-14. Fig.12a shows the C+P_4 without PAI results for the 1225°C, 1275°C and 1325°C anneals while the C_7+P_4 without PAI results are shown in Fig.12b. The C_7 XRD curves show sharper peaks than the monomer C suggesting better SPE crystal quality and this supports the lower TW values of 4350 versus 5500 and the X-TEM images in Fig.11a & b comparing C+P_4 to C_7+P_4 1325°C anneal. Fig.13 shows the XRD results for C+P_4 with a) Ge-PAI, b) Xe-PAI and c) Sb-PAI. There is no significant difference between the various PAI species but the higher the laser peak temperature the sharper the diffraction peak and therefore better crystal quality again similar to the TW trend shown in Fig. 10. Fig.14 shows the results for C_7+P_4 with a) Ge-PAI, b) Xe-PAI and c) Sb-PAI. Similar to the C with PAI results in Fig.13 the deeper amorphous layer formed by the PAI implant dominates Csub during SPE at the higher laser anneal temperature for C_7 with PAI. The calculated/modeled Csub levels are shown in Fig.15a for C+P_4 with and w/o PAI and in Fig.15b for C_7+P_4 with and w/o PAI. Without PAI the Csub level for C+P_4 is 1.21-1.25% independent of laser peak temperature and the P dopant activation Rs value is ~275 ohms/sq as shown in Fig.8. However, with PAI Csub increased to 1.42-1.5% independent of peak temperature but now the dopant activation Rs values are strongly dependent on laser peak temperature up to 1275°C as shown in Fig.8. Rs was <275 ohms/sq at 1275°C and 1325°C but degrades by 3x to 900 ohms/sq at 1175°C. For C_7+P_4 without PAI the Csub level was higher than monomer C at 1.45% but the Rs value at 1175°C was 750 ohms/sq, 1225°C was 400ohms/sq and at 1275°C or 1325°C was <275 ohms/sq. With Ge-PAI or Xe-PAI Csub was also 1.42-1.48% while Sb-PAI had the highest Csub level up to 1.52%. Again, for all the Csub results there was no clear peak temperature dependence on Csub but a significant difference between C w/o and with PAI. However, for C with PAI or all the C7 conditions the P_4 dopant activation Rs values were very temperature dependent below 1275°C. At 1175°C the Rs value was 1600 ohms/sq for C_7 with Ge-PAI and Xe-PAI but at 1275°C and above Rs was <220 ohms/sq for Sb-PAI. The calculated strain layer thickness is shown in Fig.16a for C+P_4 and Fig.16b for C_7+P_4. Note that the C strain layer is about 31nm deep for monomer C and 38nm deep for the C_7 equivalent implant condition. The Csub % depth profile based on 3 layer XRD modeling in shown in Fig.17a for C+P_4 and C_7+P_4 w/o PAI while Fig.17b for PAI+C+P_4 and Fig.17c for PAI+C_7+P_4. Without PAI, the Csub surface value for C_7 is 1.45% compared to 1.25% for monomer C. PAI neutralizes this difference and the Csub profile is determined by the deep PAI species but C_7 Csub is slightly higher by ~0.5% than monomer C.

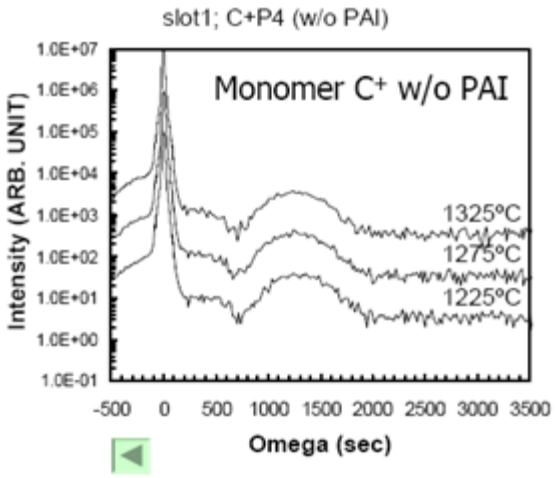

Fig.12a: HR-XRD rocking curve for $C+P_4$.

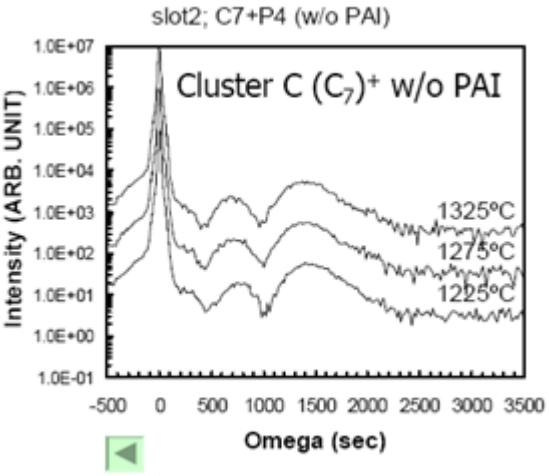

Fig.12b: HR-XRD rocking curve for C_7+P_4.

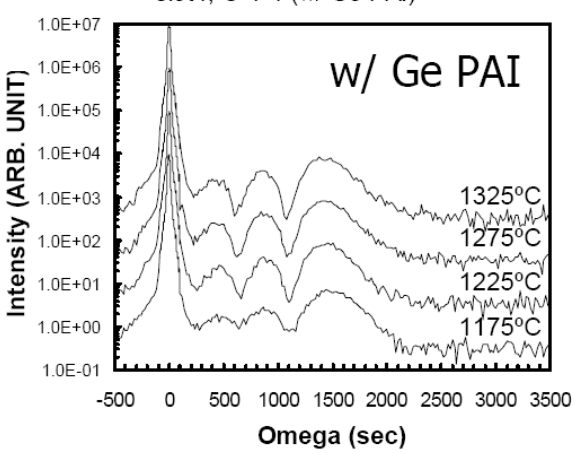

Fig.13a: HR-XRD for $C+P_4$ with Ge-PAI.

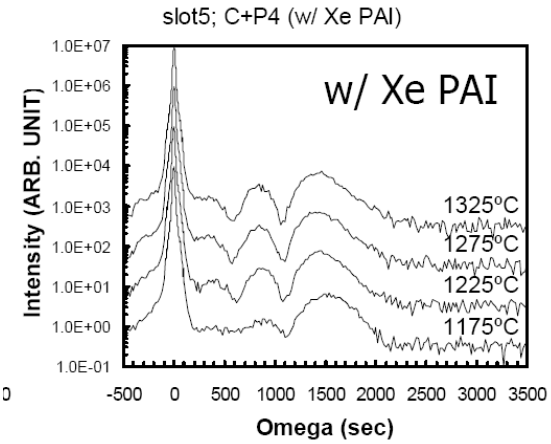

Fig.13b: HR-XRD for $C+P_4$ with Xe-PAI.

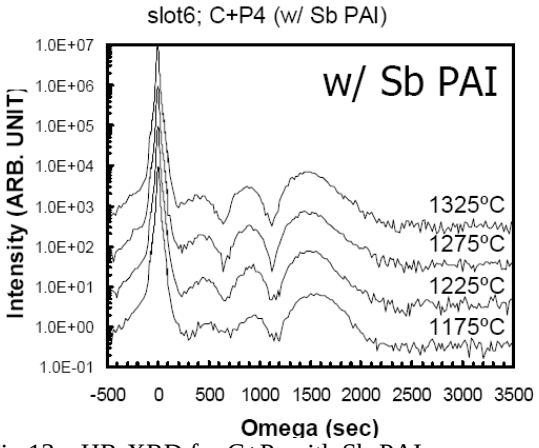

Fig.13c: HR-XRD for $C+P_4$ with Sb-PAI.

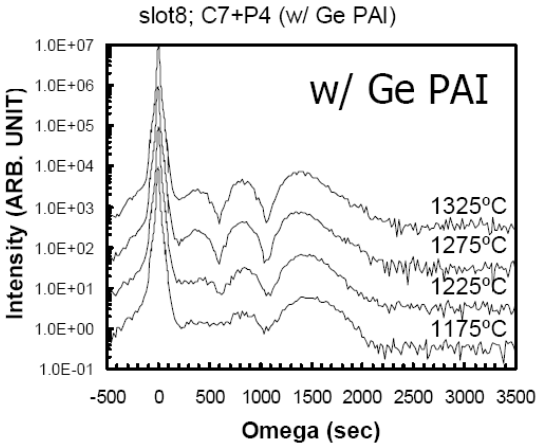

Fig.14a: HR-XRD for C_7+P_4 with Ge-PAI.

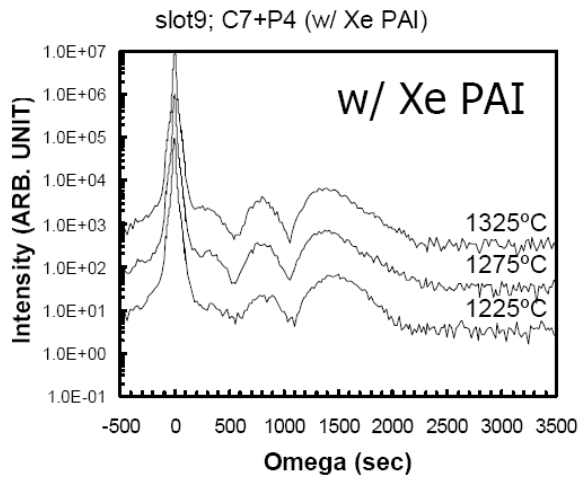

Fig.14b: HR-XRD for C_7+P_4 with Xe-PAI.

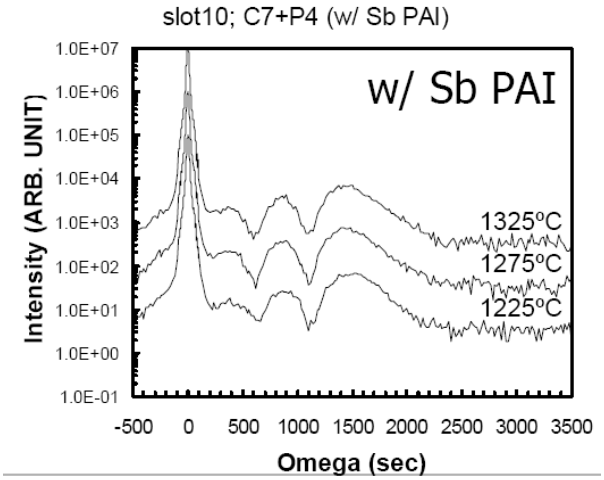

Fig.14c: HR-XRD for C_7+P_4 with Sb-PAI.

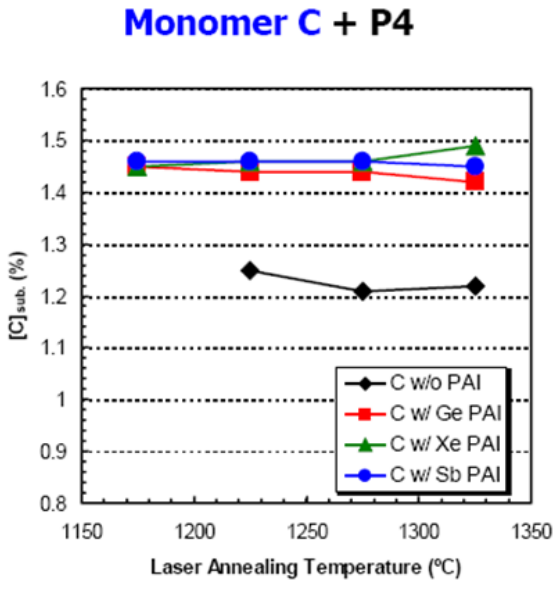

Fig.15a: Calculated Csub level for C+P_4.

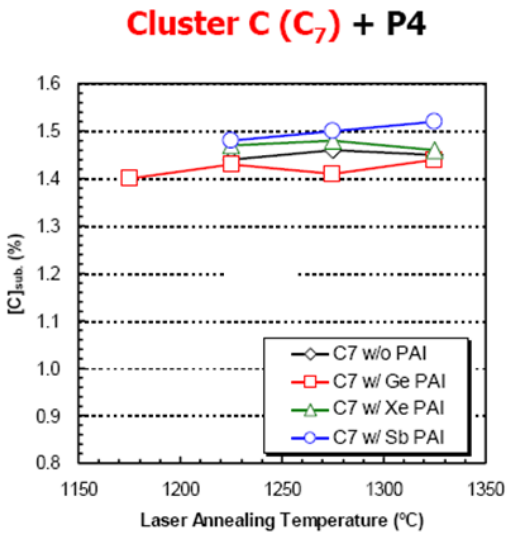

Fig.15b: Calculated Csub level for C_7+P_4.

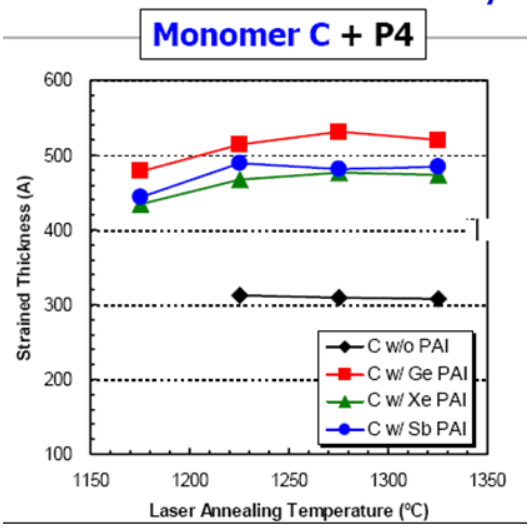

Fig.16a: Calculated strain layer thickness for C+P_4.

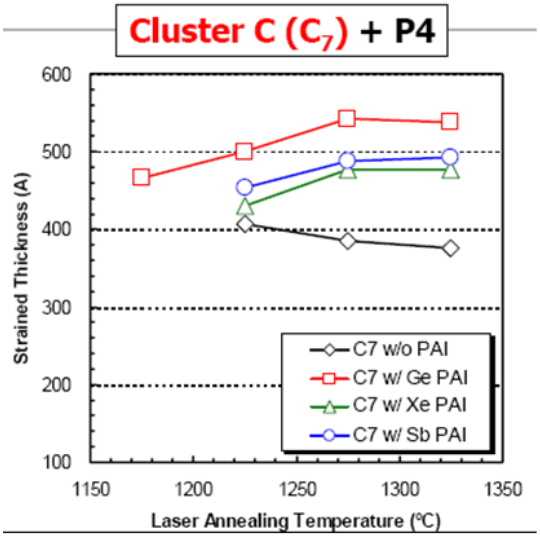

Fig.16b: Calculated strain layer thickness for C_7+P_4.

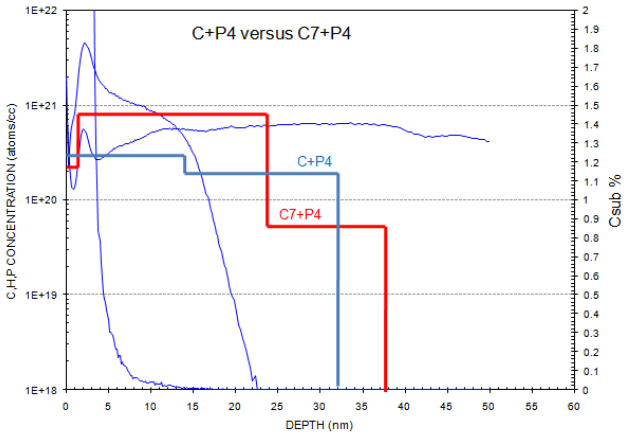

Fig.17a: Csub depth modeling for C+P_4 versus C_7+P_4.

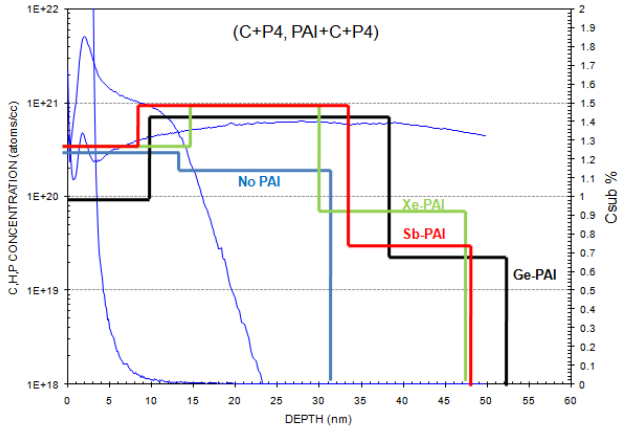

Fig.17b: Csub modeling for C+P_4 and PAI+C+P_4.

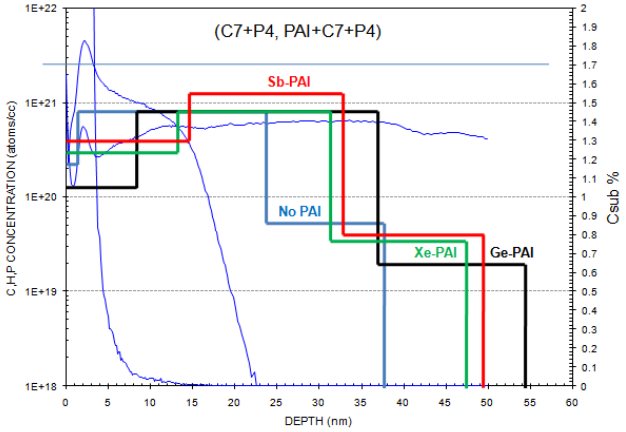

Fig. 17c: Csub modeling for C_7+P_4 and PAI+C_7+P_4.

Sekar et al. [5] reported the amorphous depth for C_7 was 35nm so our result is slightly deeper at 38nm and Maynard et al. [6] reported monomer C should also be 35nm but our result is shallower at 31nm as shown in Fig.16a&b. As shown earlier in Fig.3 the 40keV Ge-PAI at 5E14/cm2 dose amorphous layer should be 60nm deep and the strain layer thickness results for Ge-PAI+C+P_4 is 53nm and 55nm for Ge-PAI+C_7+P_4 shown in Fig. 16. The Xe-PAI and Sb-PAI at 60keV and 5E13/cm2 dose created a slightly shallower amorphous layer as shown in Fig.3 and X-TEM in Fig.2 (50nm amorphous layer) resulting in strain layer thickness of 48-49nm.

SUMMARY

We investigated n+ SiC stressor formation for the 22nm node using monomer C and C_7 implant with P_4 doping with or without Ge, Xe or Sb PAI and laser annealing with peak temperature between 1175°C to 1325°C. The best P dopant activation level (Rs=209 ohms/sq) for a Pss>4E20/cm^3 and C substitutional level (Csub=1.52%) was achieved with Sb-PAI+C_7+P_4 and 1325°C laser peak temperature but 1275°C was 2nd best. Comparing monomer C to C_7 self amorphization of C_7 after anneal resulted in lower residual implant damage as detected by TW and X-TEM. The presence of a deep amorphous layer reduced C channeling and made P dopant activation very temperature dependent below 1275°C.

ACKNOWLEDGMENTS

The authors are grateful to the support received from Dick Hockett of EAG.

REFERENCES

1] Global Foundries public announcement on July 24, 2009 that they will use eSiC for nMOS stressor at 22nm node.
2] B. Yang et al., The ECS PRiME 2008 meeting, Oct. 2008, abstract # 2416.
3]M. Bauer et al., The ECS PRiME 2008 meeting, Oct. 2008, abstract #2486.
4] Y. Liu et al., VLSI Sym. 2007, section 4A-2, p.44.
5] K. Sekar, W. Krull, T. Horsky, D. Jacobson, K. Jones ad D. Henke, Insights 2007, p. 141.
6] M. Maynard, C. Hatem, H. Gossmann, Y. Erokhin, N. Variam, S. Chen and Y. Wang, IEEE/RTP 2008, p. 147.
7] K. Sekar, W. Krull, J. Chen, S. McCoy and J. Gelpey, IEEE/RTP 2008, p. 107.
8] H. Itokawa et al., to be published SSDM-2009 paper A-3-1, Oct. 8, 2009.
9] M. Nishikawa et al., VLSI-TSA, April 2009 Taiwan.